

## De Saint-Venant equations-based model assessment in model predictive control of open channel flow

M. Xu<sup>a,\*</sup>, R.R. Negenborn<sup>b</sup>, P.J. van Overloop<sup>a</sup>, N.C. van de Giesen<sup>a</sup>

<sup>a</sup> Section of Water Resources Management, Faculty of Civil Engineering and Geosciences, Delft University of Technology, Stevinweg 1, 2628CN, Delft, The Netherlands

<sup>b</sup> Section of Marine and Transport Technology, Faculty of Mechanical, Maritime and Materials Engineering, Delft University of Technology, Mekelweg 2, 2628CD, Delft, The Netherlands

### ARTICLE INFO

#### Article history:

Received 11 July 2011

Received in revised form 3 July 2012

Accepted 5 July 2012

Available online 25 July 2012

#### Keywords:

Model predictive control

Quadratic Programming

Open channel flow

Sequential Quadratic Programming

Saint-Venant equations

### ABSTRACT

Model predictive control (MPC) is a model-based control technique that uses an optimization algorithm to generate optimal control actions. Based on the model used in optimization, MPC approaches can be categorized as linear or nonlinear. Both classes have advantages and disadvantages in terms of control accuracy and computational time. A typical linear model in open channel water management is the Integrator Delay (ID) model, while a nonlinear model usually refers to the Saint-Venant equations. In earlier work, we proposed the use of linearized Saint-Venant equations for MPC, where the model is formulated in a linear time-varying format and time-varying parameters are estimated outside of the optimization. Quadratic Programming (QP) is used to solve the optimization problem. However, the control accuracy of such an MPC scheme is not clear. In this paper, we compare this approach with an MPC scheme that uses Sequential Quadratic Programming (SQP) to solve the optimization problem. Because the estimation of the time-varying parameters is integrated in the optimization in SQP, the solutions from SQP-based MPC are expected to be superior to the solutions of QP-based approach. However, SQP can be computationally expensive. A simulation experiment illustrates that the QP-based MPC approach using a linearized Saint-Venant model has an accurate approximation of the control performance of SQP.

Crown Copyright © 2012 Published by Elsevier Ltd. All rights reserved.

### 1. Introduction

Over the last decade, model predictive control (MPC) of open channel flow has been a subject of extensive study [1–6]. MPC is a model-based control technique that uses an optimization algorithm to generate optimal control actions. Advantages of MPC are that it predicts the future system dynamics, therefore being able to take into account future known disturbances. It can also deal with constraints within the optimization. Based on the type of model used in the optimization, MPC approaches can be categorized as linear or nonlinear. The focus of MPC in open channel water management is mainly on efficient water delivery in irrigation systems, and river operations for flood or drought prevention. A common feature of the existing research is that, typically, linear models are used for predicting the system dynamics, such as the reservoir model and the classical Integrator Delay (ID) model in [1–5]. Under certain assumptions, these linear models can approximate the nonlinear system dynamics well. The MPC optimization problems when using such linear models are easy and fast to solve. Moreover, guaranteed global optimal solutions can be found.

A nonlinear model can normally include more system dynamics than a linear one. This extra information in the nonlinear model may increase the control accuracy in MPC. However, due to the use of such a nonlinear model, the optimization problem can become non-convex and hard to solve. Indeed, this is the case when using the Saint-Venant equations. Theoretically, a guarantee for finding the global optimum for nonlinear optimization cannot often be given [7]. Since the optimal action needs to be taken within a prescribed time period in real-time control, computational time is important in achieving the optimum. Unfortunately, such a nonlinear MPC scheme can be very time consuming, e.g., due to the CPU-intensive model executions for the numerical calculation of gradients of a Lagrangian function with respect to the control variables, especially in the areas where these gradients are flat. This computational complexity in MPC using such a nonlinear model was also stated by Barjas Blanco [6]. Therefore, they used a series of reservoir models instead.

Some researchers use adjoint sensitivity analysis to speed up the nonlinear optimization by analytically calculating the gradients of the Lagrangian function with respect to the control variables [8,9]. This is attractive for making such an MPC implementation feasible in real-time control, but it needs extensive analytical analysis of the nonlinear model and its derivatives beforehand. Moreover, any change to the control problem requires a new analytical derivation. For these reasons, the

\* Corresponding author. Tel.: +31 0 152782345; fax: +31 0 152785559.

E-mail address: [min.xu@tudelft.nl](mailto:min.xu@tudelft.nl) (M. Xu).

adjoint sensitivity analysis is not conducted in this paper. Instead, in [10], we proposed an MPC scheme using linearized Saint-Venant equations in a time-varying format to approximate the nonlinear dynamics. The scheme requires a much more complex discretization and mathematical formulation of the equations than the reservoir model in [6]. This MPC scheme solves the optimization problem with a standard Quadratic Programming (QP) solver, which considers the model constraints as linear.

The MPC approach in [10] is found to be the most accurate for comparison with MPC using an Integrator Delay model and a Reduced Saint-Venant model. The proposed method formulates the Saint-Venant equations as a linear time-varying state-space model. It uses a 'Forward Estimation' to estimate the time-varying parameters outside of the optimization, based on the optimal solutions over a prediction horizon from the previous control step. However, due to the lack of information at the last prediction step, the optimal solutions in the previous control step are not optimal anymore in the present step. Therefore, it is unclear what the performance of this QP-based MPC controller is. The purpose of this work is to explore the accuracy of the control procedure of [10] by comparing the results with an MPC controller that formulates Sequential Quadratic Programming (SQP) problems and solves the entire time-varying Saint-Venant equations within the optimization. According to Schittkowski [11], SQP is a state-of-the-art method for solving nonlinear programming problems. Here the MPC scheme using this method is called SQP-based MPC.

In this paper, we focus on the performance assessment of the two MPC schemes in terms of water level deviations from the target and the control actions. Because of the integrated calculation of the time-varying parameters within the optimization, the solutions from SQP-based MPC are expected to be superior to the solutions of QP-based approach, given sufficient computation time. It is the question how the two methods compare in terms of computational time and control accuracy. Regarding the control accuracy, the SQP-based MPC can be used as a benchmark. In addition, for the QP-based MPC, iterations are added between the 'Forward Estimation' and the 'Quadratic Programming' blocks, in order to compensate the influence of the lack of information at the last prediction step. Therefore, another goal of this work is to investigate the significance of this influence.

This paper is organized as follows. Section 2 describes the main components of MPC, including the open channel flow modeling and the optimization problem formulation. It summarizes the QP-based MPC scheme using the linearized Saint-Venant model and introduces the SQP-based MPC scheme. Section 3 introduces the test case used to compare the control performance between the two MPC schemes. A detailed demonstration of the results is given in Section 4 and conclusions and future research are given in Section 5.

## 2. Model predictive control of open channel flow

Model predictive control has a general structure which uses an internal model to predict the future system dynamics over a finite prediction horizon and solves a constrained optimization problem with a certain optimization algorithm. MPC uses online optimization, which means the optimization is conducted at every control time step and only the first control action over the prediction horizon is applied to the system. A typical MPC control problem in open channel water management is to maintain a water level distant downstream of a control structure at the end of the canal reach, which will also be the subject of this paper. In the following sections, we discuss the main components of MPC for such a system: internal model and optimization.

### 2.1. Open channel flow model

In order to control the open channel flow with MPC, the dynamics of the system needs to be properly defined in the internal model of the controller. Open channel flow dynamics is usually described by the Saint-Venant equations, which contain the mass and momentum conservations [12] shown in Eqs. (1) and (2):

$$\frac{\partial A_w}{\partial t} + \frac{\partial Q}{\partial x} = q_l \quad (1)$$

$$\frac{\partial Q}{\partial t} + \frac{\partial(Qv)}{\partial x} + gA_w \frac{\partial \zeta}{\partial x} + g \frac{Q|Q|}{C_z^2 R A_w} = 0 \quad (2)$$

where  $A_w$  is the wetted area [ $m^2$ ],  $Q$  is the flow [ $m^3/s$ ],  $q_l$  is the lateral inflow per unit length [ $m^3/s/m$ ],  $v$  is the average flow velocity [ $m/s$ ], which equals  $Q/A_w$ ,  $\zeta$  is the water level above the reference plane [ $m$ ],  $C_z$  is the Chezy coefficient [ $m^{1/2}/s$ ],  $R$  is the hydraulic radius [ $m$ ], which equals  $A_w/P_f$  ( $P_f$  is the wetted perimeter [ $m$ ]) and  $g$  is the gravity acceleration [ $m/s^2$ ],  $\Delta t$  is time step [ $s$ ] and  $\Delta x$  is spatial increment [ $m$ ].

According to Stelling and Duinmeijer [13], the Saint-Venant equations can be spatially discretized with staggered grids. A semi-implicit scheme is applied to the time integration, where the advection term in the momentum equation is explicitly discretized by a first-order upwind method. The friction term is linearized by using  $|Q|$  explicitly. All other terms are implicit. In this way, the Saint-Venant equations are linearized at every time step. Substituting the velocities of step  $n+1$  from the discretized version of Eq. (2) into Eq. (1), the water levels can be calculated with a tri-diagonal system, and the velocities are updated with the calculated water levels through the momentum Eq. (2). The detailed discretization of the Saint-Venant equations is included in the Appendix.

In general, there is no specific format for the model constraints in MPC. However, in QP-based MPC, the internal model is usually formulated as a linear state-space system. Due to the inter-connection between water levels and velocities, the Saint-Venant equations are approximated by a linear state-space model that is time-varying as shown in Eq. (3):

$$x^{k+1} = A^k x^k + B_u^k u^k + B_d^k d^k \quad (3)$$

where  $x$  is the state vector,  $A$  is the state matrix,  $u$  is the control input vector,  $B_u$  is the control input matrix,  $d$  is the disturbance vector,  $B_d$  is the disturbance matrix and  $k$  is the time step index. The detailed formulation of each matrix is included in the Appendix.

### 2.2. Generic MPC formulation

Typically, an MPC problem in open channel water management solves the minimization of a quadratic objective function, subject to linear or nonlinear model equality constraints and linear inequality constraints on the control inputs. The reason to use a quadratic objective function is to balance both positive and negative variations of states and control inputs, such as water level deviations from the target level and the change of controlled structure flow. The formulation can then be written for a certain control time step  $k$ :

$$\begin{aligned} \min_{x^k, U^k} J(x^k, U^k) &= \min_{x^k, U^k} \left\{ \sum_{j=0}^{n-1} [(x^{k+j+1})^T W_x x^{k+j+1}] + \sum_{j=0}^{n-1} [(u^{k+j})^T W_u u^{k+j}] \right\} \\ \text{s.t. } h_i(x^k, U^k) &= 0 \quad i = 1, \dots, m_e \\ r_i(x^k, U^k) &\leq 0 \quad i = 1, \dots, m_i \end{aligned} \quad (4)$$

where  $J$  represents a quadratic objective function,  $x^k = [x^{k+1}, \dots, x^{k+n}]^T$  and  $U^k = [u^k, \dots, u^{k+n-1}]^T$  are the states and control inputs over the prediction horizon with a length of  $n$ ,  $h_i$  and  $r_i$  are the  $i$ th

equality and inequality constraints, respectively,  $m_e$  is the number of equality constraints,  $m_i$  is the number of inequality constraints,  $W_x$  and  $W_u$  are diagonal matrices representing the weighting factors on the state  $x$  and the control input  $u$ , respectively.

In open channel flow system, typically the state  $x^{k+j+1} = \zeta^{k+j+1} - \zeta_t$  is the water level deviation from the target level ( $\zeta_t$ ) and the control input  $u^{k+j} = Q_c^{k+j} - Q_c^{k+j-1}$  is the change of structure flow, where  $Q_c$  is the controlled structure flow. The downstream water level of a canal reach is assumed controlled, and  $W_x$  only penalizes the controlled water level deviation. The equality constraints reflect the dynamics of the system, e.g. the Saint-Venant equations in this case. The structure flow  $Q_c$  is restricted typically between the minimum and maximum flows of  $Q_{c,\min}$  and  $Q_{c,\max}$  as the inequality constraints, namely  $Q_{c,\min} \leq Q_c^{k+j} \leq Q_{c,\max}$ , ( $j = 0, \dots, n-1$ ). Note that both equality and inequality constraints are over the prediction horizon  $n$ .

According to the type of model constraints, the obtained optimization problem can be solved with different solvers. For example, if the model constraints are linear, Quadratic Programming (QP) can be used. If the model constraints are nonlinear, Sequential Quadratic Programming (SQP) can be used. In this paper, Eq. (3) is a linear time-varying system with proper discretization. It is a linear approximation of partial differential equations at each time step with time-varying parameters. However, the equation is actually nonlinear over a finite horizon, which exactly needs to be considered in MPC as the internal model. In the following sections, we discuss two methods to estimate the time-varying parameters in MPC.

### 2.3. QP-based model predictive control

QP-based MPC is intended to solve a quadratic optimization problem subject to linear constraints. Xu et al. [10] approximates the linear time-varying Saint-Venant model over the prediction horizon as a linear model. Fig. 1 shows the work flow of the QP-based MPC controlling a water system. In this MPC scheme, the time-varying parameters of  $A^k$ ,  $B_u^k$  and  $B_d^k$  are calculated outside of the optimization solver and estimated through a 'Forward Estimation' procedure. 'Forward Estimation' simulates the Saint-Venant equations over a finite prediction horizon based on the previous optimal solutions which, in this paper, are the optimal gate flows over the prediction horizon.

However, due to the control step change from  $k-1$  to  $k$ , the optimal flow of the last prediction step is missing. Therefore, the optimal solutions at step  $k-1$  are not optimal any more at step  $k$  with the new system information of the last prediction step. This lack of system information is severe for the very first control step when no previous optimal solutions are available at all. In order to handle this drawback and increase the control accuracy, iterations between the blocks of 'Forward Estimation' and 'Quadratic Programming' can be included in the procedure. In practice, not all the water levels are measured along a canal. Therefore, a standard Kalman filter [14] is used to estimate the unmeasured water levels with a limited number of measurements.

When the model Eq. (3) over a prediction horizon is substituted into the objective function (4) with calculated  $A^k$ ,  $B_u^k$  and  $B_d^k$ , the optimization problem can be written as:

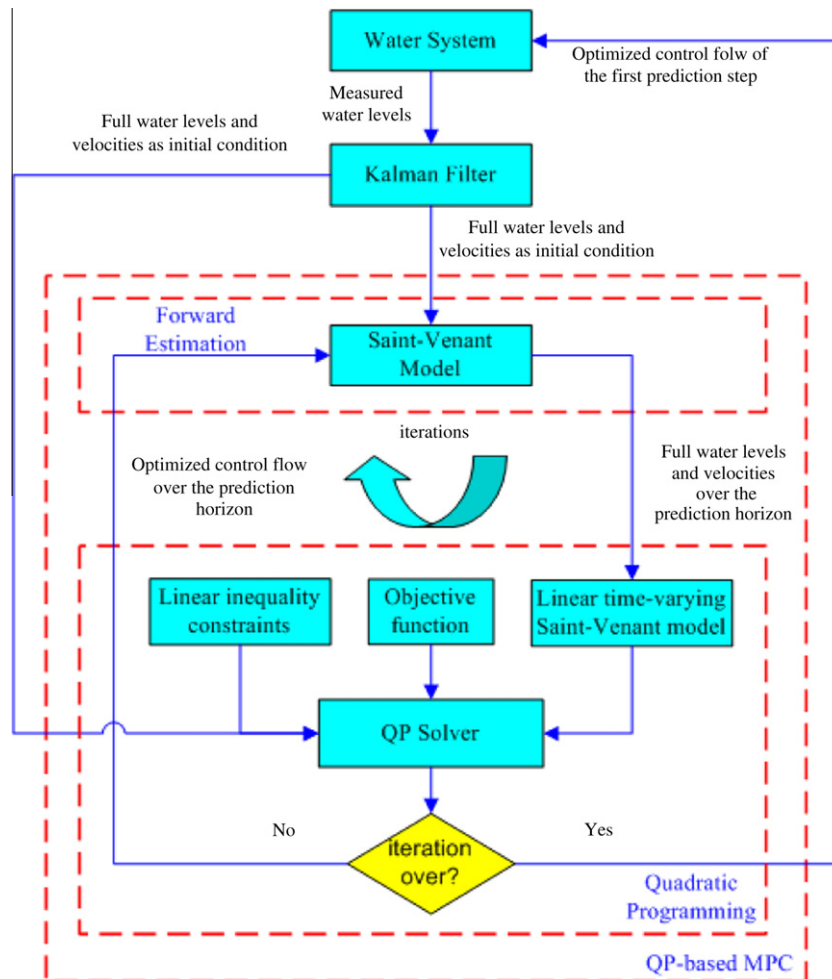


Fig. 1. QP-based MPC controlling a water system.

$$\min_{U^k} J(U^k) = \min_{U^k} \left( \frac{1}{2} (U^k)^T H^k U^k + (f^k)^T U^k + g_c \right) \quad (5)$$

$$s.t. Q_{c,\min} \leq Q_c^{k+j} \leq Q_{c,\max} \quad j = 0, \dots, n-1$$

where  $H$  is the Hessian matrix,  $f$  is the Jacobian matrix and  $g_c$  is a constant matrix.

Because the constrained model is linear with pre-determined and fixed time varying parameters of  $A^k$ ,  $B_u^k$  and  $B_d^k$ , the Hessian and the Jacobian can be analytically calculated with one model run over the prediction horizon [3]. Therefore, there is no need for extra model executions for the gradient comparing to numerical calculation, which saves a large amount of computational time, especially when iterations are used within the optimization. But the MPC procedure does need  $(n_{\text{iter}} + 1) \times 2n$  model executions for the 'Forward Estimation' to estimate the time varying parameters and for the calculation of the Hessian and Jacobian, where  $n_{\text{iter}}$  is the number of iterations between the 'Forward Estimation' and 'Quadratic Programming'. The optimization problem of Eq. (5) is a typical Quadratic Programming problem, which is in our case solved by the standard MATLAB function 'quadprog' [15].

#### 2.4. SQP-based model predictive control

In SQP-based MPC approach, a specific model format is not required. However, because of the linear time-varying state-space model setup for the QP-based MPC, this model setup is also applied in a SQP-based MPC scheme. Fig. 2 illustrates the work flow of an SQP-based MPC controlling the same water system as in Section 2.3. Compared to QP-based MPC, the 'QP-based MPC' block in Fig. 1 is replaced by 'SQP-based MPC'. In this scheme, the entire model over a finite prediction horizon is integrated in a sequence of QP sub-problems, which are solved by a QP optimization solver until the objective function value converges. Because the time-varying parameters are calculated internally in the optimization, the solutions are guaranteed to be optimal.

In Sequential Quadratic Programming (SQP), the objective function is required to have a second order derivative and the

constraints are required to be continuously differentiable. SQP formulates a sequence of QP sub-problems based on the Hessian approximation of the Lagrangian function by taking the second order Taylor expansion of the Lagrangian function, and uses an iterative way to solve the QP sub-problems. In this paper, the MATLAB function 'fmincon' [15–18] is used to solve the SQP problem. However, for the sake of facilitation of explaining the number of model executions required (which is related to the computational time), we provide some relevant equations of SQP.

SQP is based on the Lagrangian function shown in Eq. (6) with the Lagrange multipliers on the model constraints.

$$L(X^k, U^k, \Lambda^k, N^k) = J(X^k, U^k) + \sum_{i=1}^{m_e} \Lambda_i^k h_i(X^k, U^k) + \sum_{i=1}^{m_i} N_i^k r_i(X^k, U^k) \quad (6)$$

where  $L$  is the Lagrangian function,  $\Lambda_i^k = [\lambda_i^{k+1}, \dots, \lambda_i^{k+n}]^T$  and  $N_i^k = [\mu_i^{k+1}, \dots, \mu_i^{k+n}]^T$  are the Lagrange multipliers.

The QP sub-problems at control step  $k$  are formulated according to Eq. (7) by taking the second order Taylor expansion of the Lagrangian function. The solutions of the QP sub-problems  $S$  are used to formulate the next iteration until the objective function values converge.

$$\min_{X^k, U^k, \Lambda^k, N^k} L(X^k, U^k, \Lambda^k, N^k) = \min_{S^k} \left( \frac{1}{2} (S^k)^T H_{L,p}^k S^k + (f_{L,p}^k)^T S^k + g_{L,p}^k \right) \quad (7)$$

$$s.t. \quad h_i(X_p, U_p) + \nabla_X h_i(X_p, U_p) s_1 + \nabla_U h_i(X_p, U_p) s_2 = 0, \quad i = 1, \dots, m_e$$

$$r_i(X_p, U_p) + \nabla_X r_i(X_p, U_p) s_1 + \nabla_U r_i(X_p, U_p) s_2 \leq 0, \quad i = 1, \dots, m_i$$

where  $H_{L,p}^k$  is the Hessian matrix of the Lagrangian function at  $(X_p^k, U_p^k)$ ,  $f_{L,p}^k$  is the Jacobian matrix of the Lagrangian function at  $(X_p^k, U_p^k)$ ,  $g_{L,p}^k$  is the constant matrix,  $S^k$  is the search direction containing  $S_1^k = X_{p+1}^k - X_p^k$ , and  $S_2^k = U_{p+1}^k - U_p^k$ . Note that the subscript  $p$  represents the iteration index in SQP.

Because of the difficulty in analytically calculating the gradient of the Lagrangian function, a numerical method is often used to estimate the gradient by executing the prediction model. Forward difference is one of the numerical methods for the estimation by assuming a small perturbation  $\delta$  on the state or the control input, as described in Eq. (8):

$$\nabla_X L(X_p^k, U_p^k, \Lambda_p^k, N_p^k) = \left[ \frac{L_{X_p^{k+1}+\delta} - L_{X_p^k}}{\delta}, \frac{L_{X_p^{k+2}+\delta} - L_{X_p^{k+1}}}{\delta}, \dots, \frac{L_{X_p^{k+n}+\delta} - L_{X_p^{k+n-1}}}{\delta} \right]^T \quad (8)$$

$$\nabla_U L(X_p^k, U_p^k, \Lambda_p^k, N_p^k) = \left[ \frac{L_{U_p^{k+1}+\delta} - L_{U_p^k}}{\delta}, \frac{L_{U_p^{k+2}+\delta} - L_{U_p^{k+1}}}{\delta}, \dots, \frac{L_{U_p^{k+n-1}+\delta} - L_{U_p^{k+n-2}}}{\delta} \right]^T$$

The Lagrange multipliers in calculating the gradient of the Lagrangian function can be obtained through the Karush–Kuhn–Tucker (KKT) conditions shown in Eq. (9). KKT conditions are the first order necessary optimality conditions that need to be fulfilled for nonlinear optimization [19,20]. It is obtained by taking the partial derivative of the Lagrangian function with respect to  $X^k$ ,  $U^k$ ,  $\Lambda^k$  and  $N^k$ .

$$\begin{cases} \nabla L(X_p^k, U_p^k, \Lambda_p^k, N_p^k) = \nabla_X J(X_p^k, U_p^k) + \nabla_U J(X_p^k, U_p^k) \\ + \sum_{i=1}^{m_e} \Lambda_{i,p}^k \nabla_X h_i(X_p^k, U_p^k) + \sum_{i=1}^{m_i} N_{i,p}^k \nabla_U r_i(X_p^k, U_p^k) = 0 \\ \Lambda_{i,p}^k h_i(X_p^k, U_p^k) = 0 \\ N_{i,p}^k \geq 0 \end{cases} \quad (9)$$

In order to numerically calculate the Jacobian matrix of the Lagrangian function,  $n(2n+1)$  model runs are required. These model runs include  $n$  runs to calculate the Lagrangian function values of  $L_{X^{k+1}}, \dots, L_{X^{k+n}}$  and  $L_{U^k}, \dots, L_{U^{k+n-1}}$  and  $2 \times n \times n$  additional runs to calculate the Lagrangian function values with small perturbation on each of the variables of state  $X$  and control input  $U$ , namely  $L_{X^{k+1}+\delta}, \dots, L_{X^{k+n}+\delta}$  and  $L_{U^k+\delta}, \dots, L_{U^{k+n-1}+\delta}$ . Because all the model variables over the prediction horizon in  $X$  and  $U$  are dependent, a small

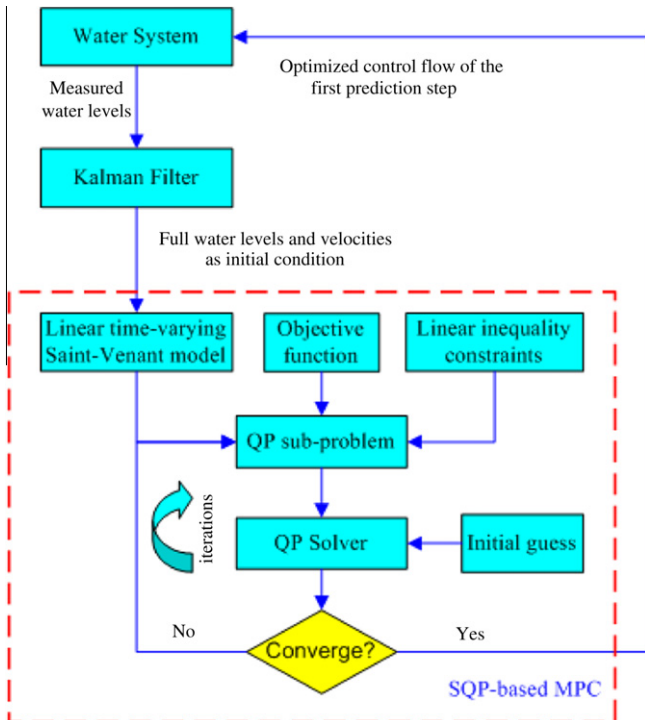


Fig. 2. SQP-based MPC controlling a water system.



perturbation on one variable will change the model constraints and influence all Lagrangian function values. Thus, the model needs to be executed over the prediction horizon  $n$  for each small perturbation of the  $2n$  variables in order to calculate the Jacobian matrix.

For the Hessian matrix, Quasi-Newton method is used to calculate the Hessian approximation. The Broyden–Fletcher–Goldfarb–Shanno (BFGS) method is one of the most popular algorithms to update the Hessian approximation based on the Jacobian matrix [19]. Therefore, there is no need for extra model executions to calculate the Hessian matrix of the Lagrangian function.

In total,  $n(2n + 1)$  model runs are required for each of the iterations in the nonlinear optimization with the forward difference method.

### 3. Test case

In order to assess the performance of the QP-based MPC scheme using the linearized Saint-Venant model in comparison with the SQP-based MPC scheme, we will perform simulation experiments. Fig. 3 describes a test canal reach and includes all the geometric parameter values. In the test case, we assume no lateral flows and try to control the downstream water level of the canal reach at  $-3.2$  m MSL (mean sea level) by operating the downstream gate with a maximum flow of  $4 \text{ m}^3/\text{s}$ , given an upstream inflow disturbance. Fig. 4 shows the inflow disturbance scenario, involving large and frequent variations. The discharges are above the maximum downstream gate flow in certain periods.

Two simulation experiments are setup to compare the QP-based and SQP-based MPC schemes. Figs. 5 and 6 show the procedures. In experiment (a) (Fig. 5), both MPC schemes use the same information from the water system, and only the optimal control actions from SQP-based MPC are sent back to the water system. This experiment illustrates the controllers' behavior with different prediction models in terms of the calculation of time-varying parameters. In experiment (b) (Fig. 6), both QP-based MPC and SQP-based MPC form their own loops with the water systems. The two water systems start from the same initial condition. This experiment is intended to show the influence of the controllers on the total water system loop. In addition, according to the QP-based MPC scheme shown in Fig. 1, different numbers of iterations are tested in each MPC implementation, especially for the first control step when no previous control information is available for calculating the time-varying parameters of the state-space model.

Each experiment covers a simulation period of 20 h with a simulation time step of 2 s. The gate is operated every 4 min using the optimal control action. The reach is discretized in 500 segments, resulting in 500 water level states. A Kalman filter is implemented to estimate the unmeasured water levels and velocities as the initial condition of the model constraints based on the measured water levels at the upstream and downstream side of the reach (details of the Kalman filter are in [10]). The optimization problem in this case is only subject to the Saint-Venant equations and there

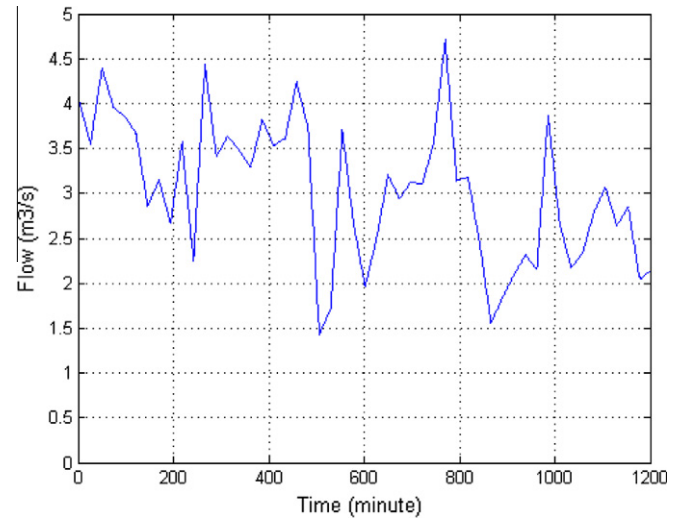


Fig. 4. Upstream inflow disturbance scenario.

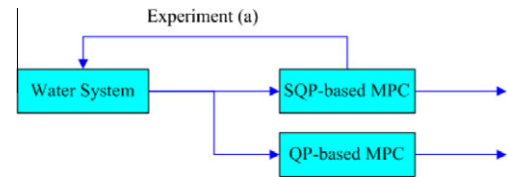


Fig. 5. Experiment of controller behavior.

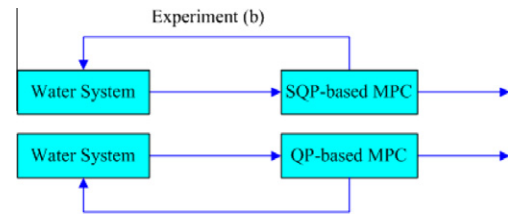


Fig. 6. Experiment of control influence on the water system.

is only one structure in control. Therefore, the number of equality constraints ( $m_e$ ) and the number of inequality constraints ( $m_i$ ) both equal to 1.

### 4. Results

In this section, we perform the experiments described in the previous section to assess the performance of the QP-based and SQP-based MPC schemes. In addition, we will provide an analysis of the computational time requirements.

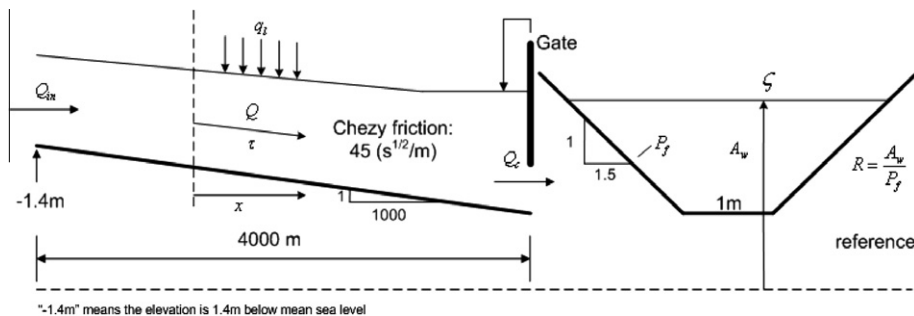


Fig. 3. Canal reach schematization.

#### 4.1. Results of control performance

##### 4.1.1. Experiment of controller behavior

Before starting experiment (a), it is necessary to analyze the convergence of the objective function values of the QP-based MPC scheme using the linearized Saint-Venant model, since iterations between the 'Forward Estimation' and 'QP solver' are used to increase the model accuracy. Over the iterations, the performance is expected to increase, as the unknown information from the previous optimization is updated. Fig. 7 shows this convergence of the objective function values at control steps 1, 13, 67, 115 and 193, where upstream inflows are above the maximum downstream control flow and the control limits may be reached. At these control steps, the upstream inflows in the prediction also change significantly, as is illustrated in Fig. 4. Note that the first objective function values in Fig. 7 are without iterations. It is clear that the objective function values converge after a certain number of iterations. But iterations only have significant influence for the very first control step, while the influence on the rest of the control steps is negligible. Fig. 8 also shows the evolution of predicted

water levels and gate flows of QP-based MPC over 30 iterations at the first control step. The evolution results are similar to Fig. 7 and show a fast convergence.

A direct indicator to compare the behavior of the controllers is to analyze the control goal of minimizing the objective function values. Fig. 9 shows the results of experiment (a). Because of the lack of previous optimal information in the QP-based MPC scheme, especially at the very first control step, the figure also plots the result of this MPC scheme with 10 iterations between the 'Forward Estimation' and 'QP solver' at the first control step. A maximum of 10 initial iterations is taken as tests showed that taking a larger number of iterations does not alter the solutions any further (Fig. 7). Fig. 9 shows that SQP-based MPC has relatively low costs per control step over the prediction horizon and outperforms the QP-based MPC in that sense. The difference between the objective function values of the two MPC schemes shows that the lack of information from the previous control step does influence the control performance, especially for the very first control step, oscillations occur due to the complete ignorance of the previous information at the beginning. But the influence vanishes quickly

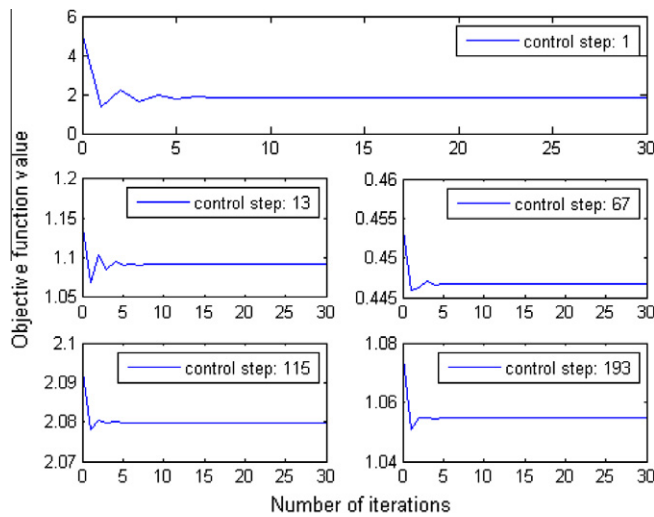


Fig. 7. Convergence of objective function values of the QP-based MPC scheme at control steps 1, 13, 67, 115, and 193.

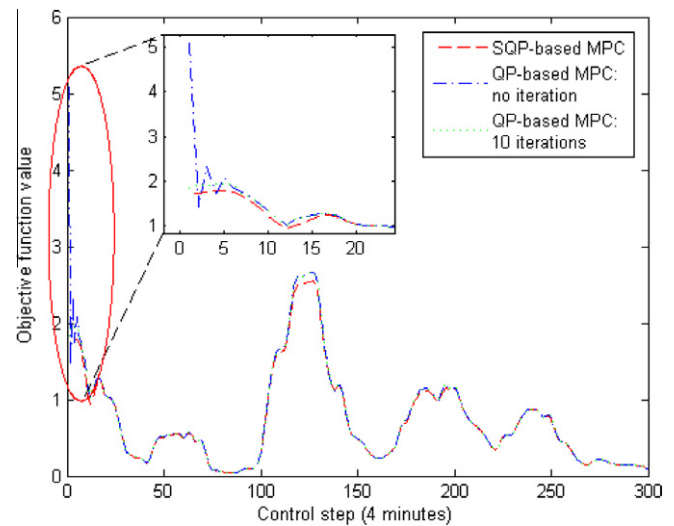


Fig. 9. Comparison of objective function values between SQP-based MPC and QP-based MPC (10 iterations are only applied at the first control step).

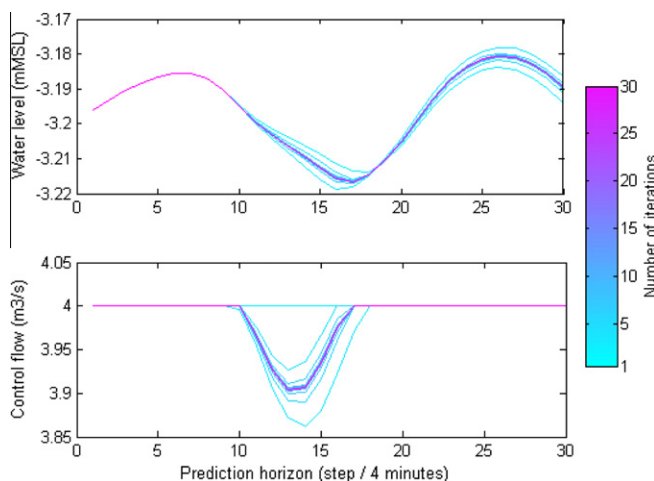


Fig. 8. Evolution of the predicted water levels and discharges of QP-based MPC over 30 iterations at the first control step.

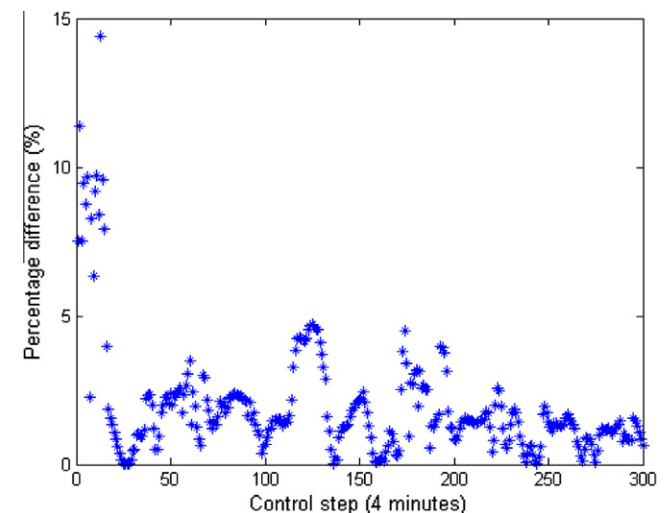


Fig. 10. Percentage difference in objective function values between SQP-based MPC and QP-based MPC with 10 initial iterations in experiment (a).

as the simulation proceeds. On the other hand, the QP-based MPC can follow the SQP-based MPC performance trajectory very well.

Moreover, there is a maximum of only 14.39% difference in the objective function values between SQP-based MPC and QP-based MPC with 10 initial iterations, shown in Fig. 10. The percentage is calculated by taking the difference of their objective function values divided by the objective function value of the SQP-based MPC scheme. The larger differences mainly happen at the beginning of the simulation, where many flow constraints are activated, but no previous information is available as will be shown in Fig. 12 later on. Although the control flow also reaches the constraints in the simulation afterwards, for example at about 800 min shown in Fig. 12, the percentage difference between the two MPC schemes is small (<5%) due to the previously available information (at about control step 200).

#### 4.1.2. Experiment of control influence on the water system

After assessing the behavior of the controllers in experiment (a), it is necessary to analyze their control influence on the water systems over a full simulation. Regarding the control performance, the

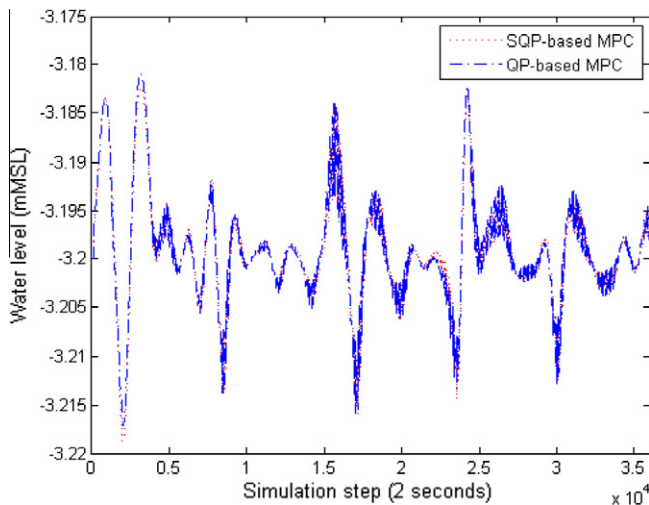


Fig. 11. Controlled water levels in SQP-based MPC and QP-based MPC without iterations.

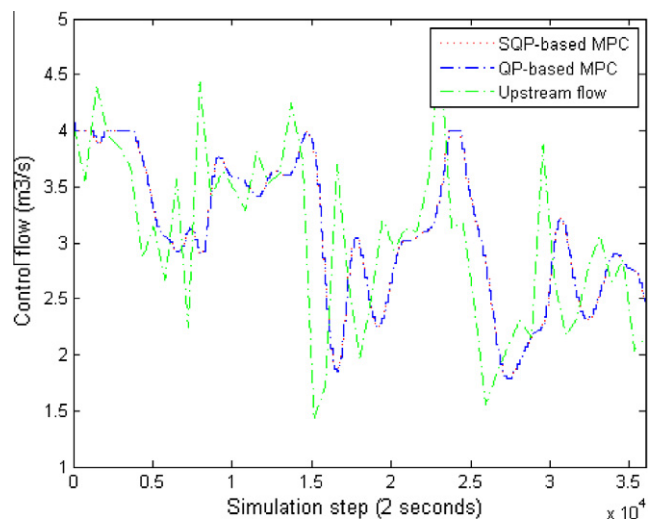


Fig. 12. Controlled discharge in SQP-based MPC and QP-based MPC without iterations (upstream inflow is plotted to indicate the downstream flow trends).

first indicators are the controlled water level and discharge evolution over the simulation horizon, shown in Figs. 11 and 12 for both MPC schemes, respectively. Both controllers can control the water levels very close to the target, and the system behavior using these two controllers is very similar. The water level oscillations that are visible in Fig. 11 are realistic and caused by the discrete steps that the controller takes every 4 min, while the flow dynamics is simulated using a 2 s time interval. The maximum control flow of 4 m<sup>3</sup>/s is reached several times during the whole simulation as shown in Fig. 12.

The performance of the controlled water levels and discharges can also be indicated through quantitative performance indicators, such as the Maximum Absolute Value (MAE) indicating the percentage of maximum water level deviation from the target and the Integrated Absolute Discharge Change (IAQ) calculated by the integral of the absolute flow changes over the simulation minus the absolute flow difference of the first and last simulation steps [21]. IAQ reflects the tear and wear of the gate over the whole simulation. The comparison of the two MPC schemes using these indicators is shown in Table 1. As can be seen, the differences in control performance between the schemes are small. Due to the higher model accuracy, SQP-based MPC has slightly lower values for the MAE and IAQ indicators, which indicates slightly better performance.

#### 4.2. Results of computational time

Computational time is important for real-time control implementation. Before the next control time step is reached, the optimization results should be available. Table 2 shows the computational time of different components in both MPC executions. According to the MPC procedures in Figs. 1 and 2, the 'total time per control step' represents the average computational time from 'water system' to 'water system' through 'Kalman filter' and 'MPC' block. The 'control time' is the specific time for the control generation in 'MPC' block. The 'model calls in control' represents the time of model simulations within the 'MPC' block. For QP-based MPC, the 'model calls in control' includes the time of calling the model in the 'Forward Estimation' and the controller, while for SQP-based MPC it is the time of calling the model in the SQP optimization. The calculation of both MPC schemes was on a 64-bit computer with an 8 Gb internal memory.

From Table 2, it follows that 99.37% of the total computational time in SQP-based MPC is used to generate the control actions,

Table 1

Performance indicators of both SQP-based MPC and QP-based MPC.

	Maximum absolute value (MAE <sup>*</sup> ) (%)	Integrated absolute discharge change (IAQ) (m <sup>3</sup> /s)
SQP-based MPC	−0.55	13.52
QP-based MPC	−0.60	13.55

\* MAE is negative because the target level is negative.

Table 2

Computational time components in both QP-based MPC and SQP-based MPC executions.

	SQP-based MPC	QP-based MPC
Total time per control step (s)	1761.25	54.39
Control time (s)	1750.14	44.40
Model calls in control (s)	1748.44	2.48

**Table 3**  
Number of model executions per control step in QP-based MPC and SQP-based MPC.

	QP-based MPC		SQP-based MPC	
	No iteration	Five iterations	$n_{iter}$ iterations	–
Number of model executions	$2n$	$(5 + 1) \times 2n$	$(n_{iter} + 1) \times 2n$	$n(2n + 1) \times \bar{n}_{iter}$

while 99.9% of the control actions calculation time is spent on the model executions within the optimization. This illustrates the importance for reducing the total number of model executions and speeding up the model computations. It is noted that the ‘control time’ and the ‘model calls in control’ do not include the time of Kalman filtering.

Moreover, there exist large computational time differences between the two MPC executions. Since the actual control time step is 4 minutes, the table indicates that the optimization time of SQP-based MPC is unacceptable in this case, while the implementation of QP-based MPC is possible and 2 or 3 iterations can even be allowed. The time of ‘model calls in control’ is not the major time consumption in QP-based MPC and most of the computational time is spent on the large matrix multiplications in order to build up the Hessian and Jacobian over the prediction, according to Xu et al. [10].

Because model calling takes most of the computational time in SQP-based MPC, it is interesting to analyze the number of model executions. Table 3 compares the number of model executions per control step of the two MPC schemes, which is a function of the number of iterations  $n_{iter}$  and the prediction horizon  $n$ . For the QP-based MPC,  $n_{iter}$  is the number of iterations between the ‘Forward Estimation’ and ‘Quadratic Programming’ blocks. For SQP-based MPC, the number of iterations per control step is taken as an average number of iterations over the full control steps ( $\bar{n}_{iter}$ ).

It should be noticed that the model execution in QP-based MPC only occurs in the ‘Forward Estimation’ and preparation of Hessian and Jacobian matrices buildup over the prediction horizon. Therefore, the number of executions increases linearly with the number of iterations between the ‘Forward Estimation’ and ‘Quadratic Programming’. Because the Hessian and Jacobian matrices are pre-calculated, there is no need to execute the model within the QP optimization, although QP iteratively solves the optimization prob-

lem. Fig. 13 shows the number of iterations used in the SQP in SQP-based MPC. There are  $\bar{n}_{iter} = 45.86$  iterations per control step on average, and every iteration requires  $n(2n + 1)$  model calls to calculate the Hessian approximation and the Jacobian matrices. For that reason, the computational difference between the two MPC schemes is significant.

## 5. Conclusions and future research

In this paper, a comparison has been made between QP-based and SQP-based MPC schemes for control of open channel flow that can be described by 1-dimensional Saint-Venant equations. Two experiments were conducted for testing the behaviors of controllers and their influence on the water systems. Both MPC schemes presented in this paper can control the water system very well. Due to the integrated calculation of the time-varying parameters of the Saint-Venant equations, more accurate prediction model is achieved in SQP-based MPC. Furthermore, SQP-based MPC achieves better control performance regarding the minimization of the objective function. On the other hand, SQP-based MPC is more computationally expensive. The QP-based MPC using the linearized Saint-Venant equations was tested in a single canal reach in this paper. However, in general, as the complexity of the problem increases, the computational time will increase accordingly when the same model accuracy (spatial discretization) is reached.

In QP-based MPC using linearized Saint-Venant model, iterations between the ‘Forward Estimation’ and ‘Quadratic Programming’ can improve the control results. But the improvement is only significant at the very first control step, when there is no previous optimal information at all and many constraints are active. The influence of this lack of previous optimal information dies out quickly as the simulation proceeds and the control results converge fast over the iterations. As a benchmark for control performance, the results of SQP-based MPC show that the procedure of QP-based MPC with the ‘Forward Estimation’ is an effective and efficient way to deal with nonlinearity of the model constraints.

This paper also provides an interesting finding that model executions take 99.9% of the control time in the optimization of SQP-based MPC. This suggests a working direction for SQP-based MPC in the future regarding reducing the total number of model executions and speeding up the model calculations, for example, the adjoint method. In addition, switching all the calculations to low level programming will also decrease the computational time significantly, since the matrix inverse in the model calculation takes much time in MATLAB calculation. Because of the non-convexity of the optimization, there is no guarantee of global optimum in nonlinear optimization. Once the computational burden of SQP-based MPC optimization is conquered, a multi-start method, a number of SQP-based MPC executions with multiple initial values, can be implemented to increase the chance of reaching the global optimum.

More practically, another future research direction regarding MPC is to analyze the influence of future uncertainty on the proposed QP-based MPC procedure. For example, what is predicted in the previous step does not happen or what is not predicted in the previous step does happen, etc. Unlike the theoretical work in this paper, which assumes perfect predictions, real world implementations have to deal with these changing predictions.

## Acknowledgement

This research was supported partly by an IBM 2010–2011 Ph.D. Fellowship Award and partly by the VENI project “Intelligent multi-agent control for flexible coordination of transport hubs” (project 11210) of the Dutch Technology Foundation STW.

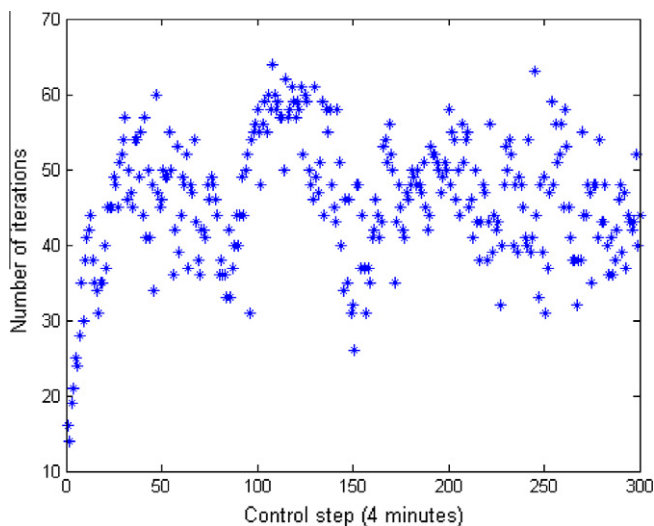


**Fig. 13.** Number of iterations used in SQP optimization.



## Appendix A. Discretization of the Saint-Venant equations and formulation as linear time-varying state-space model

The depth-averaged Saint-Venant equations are as follows:

$$\frac{\partial A_w}{\partial t} + \frac{\partial Q}{\partial x} = q_i \quad (A.1)$$

$$\frac{\partial Q}{\partial t} + \frac{\partial(Qv)}{\partial x} + gA_w \frac{\partial \eta}{\partial x} + g \frac{Q|Q|}{C_z^2 \cdot R \cdot A_w} = 0 \quad (A.2)$$

The equations can be discretized with staggered grids in space and semi-implicit for time integration as (the advection term in (A.4) is associated with the positive flow):

$$\frac{A_{w,i}^k - A_{w,i}^{k-1}}{\Delta t} = \frac{Q_{i-1/2}^k - Q_{i+1/2}^k}{\Delta x} + q_{l,i}^k \quad (A.3)$$

$$\begin{aligned} \frac{v_{i+1/2}^{k+1} - v_{i+1/2}^k}{\Delta t} + \frac{1}{\bar{A}_{w,i+1/2}^k} \left( \frac{\bar{Q}_{i+1}^k v_{i+1/2}^k - \bar{Q}_i^k v_i^k}{\Delta x} - v_{i+1/2}^k \frac{\bar{Q}_{i+1}^k - \bar{Q}_i^k}{\Delta x} \right) \\ + g \frac{\zeta_{i+1}^{k+1} - \zeta_i^{k+1}}{\Delta x} + g \frac{v_{i+1/2}^{k+1} |v_{i+1/2}^k|}{C_z^2 \cdot R_{i+1/2}^k} = 0 \end{aligned} \quad (A.4)$$

where

$$\bar{Q}_i^k = \frac{Q_{i+1/2}^k - Q_{i-1/2}^k}{2}, \bar{A}_{w,i+1/2}^k = \frac{A_{w,i+1}^k - A_{w,i}^k}{2} * v_i^k = \begin{cases} v_{i-1/2}^k (\bar{Q}_i^k \geq 0) \\ v_{i+1/2}^k (\bar{Q}_i^k < 0) \end{cases}$$

The discrete Saint-Venant equations are solved through a tri-diagonal format, if Eq. (A.4) is substituted into (A.3). The tri-diagonal format can then be re-formed in Eq. (A.5). The last equation is intended to create the change of structure flow  $\Delta Q_c$  as the control input for optimization. By multiplying the inverse of the first matrix on both sides of Eq. (A.5), it gives the linear time varying state-space model format.

$$\begin{aligned} \begin{bmatrix} a_{1,1}^k & a_{1,2}^k & 0 & 0 & 0 & 0 \\ a_{2,1}^k & a_{2,2}^k & a_{2,3}^k & 0 & 0 & 0 \\ 0 & \ddots & \ddots & \ddots & 0 & 0 \\ 0 & 0 & a_{l-1,l-2}^k & a_{l-1,l-1}^k & a_{l-1,l}^k & 0 \\ 0 & 0 & 0 & a_{l,l-1}^k & a_{l,l}^k & \frac{\Delta t}{\Delta x T_{w,l}^k} \\ 0 & 0 & 0 & 0 & 0 & 1 \end{bmatrix} \begin{bmatrix} \zeta_1^{k+1} \\ \zeta_2^{k+1} \\ \vdots \\ \zeta_{l-1}^{k+1} \\ \zeta_l^{k+1} \\ Q_c^{k+1} \end{bmatrix} \\ = I_{l+1,l+1} \begin{bmatrix} \zeta_1^k \\ \zeta_2^k \\ \vdots \\ \zeta_{l-1}^k \\ \zeta_l^k \\ Q_c^k \end{bmatrix} + \begin{bmatrix} 0 \\ \vdots \\ 0 \\ 1 \end{bmatrix} \Delta Q_c^{k+1} \\ + \begin{bmatrix} \frac{\Delta t}{\Delta x T_{w,1}^k} & 0 & 0 & 0 & \frac{\Delta t}{\Delta x T_{w,1}^k} \\ 0 & \frac{\Delta t}{\Delta x T_{w,2}^k} & 0 & 0 & 0 \\ \vdots & \vdots & \ddots & \ddots & \vdots \\ 0 & 0 & 0 & \frac{\Delta t}{\Delta x T_{w,l}^k} & 0 \\ 0 & 0 & 0 & 0 & 0 \end{bmatrix} \begin{bmatrix} -b_1^k \\ b_1^k - b_2^k \\ \vdots \\ b_{l-2}^k - b_{l-1}^k \\ b_{l-1}^k \\ Q_{in}^{k-1} \end{bmatrix} \quad (A.5)$$

where  $T_{w,i}$  is the top width at  $i$ th discrete point,  $Q_{in}$  is the upstream inflow, which is assumed as known disturbance.

$$a_{i,i-1}^k = -\frac{\Delta t}{\Delta x T_{w,i}^k} A_{w,i-1}^k f u_{i-1/2}^k, i = 2, \dots, l$$

$$a_{i,i+1}^k = -\frac{\Delta t}{\Delta x T_{w,i}^k} A_{w,i}^k f u_{i+1/2}^k, i = 1, \dots, l-1$$

$$a_{i,i}^k = 1 + \frac{\Delta t}{\Delta x T_{w,i}^k} \left( A_{w,i-1}^k f u_{i-1/2}^k + A_{w,i}^k f u_{i+1/2}^k \right), i = 1, \dots, l$$

$$b_i^k = A_{w,i}^k r u_{i-1/2}^k + q_{l,i}^{k+1}, i = 1, \dots, l-1$$

$$\begin{aligned} f u_{i+1/2}^k &= \frac{g \Delta t}{\Delta x \left( 1 + g \frac{|v_{i+1/2}^k|}{C_z^2 R_{i+1/2}^k} \right)}, \\ r u_{i+1/2}^k &= \frac{-\frac{1}{A_{w,i+1/2}^k} \left( \frac{\bar{Q}_{i+1}^k v_{i+1/2}^k - \bar{Q}_i^k v_i^k}{\Delta x} + v_{i+1/2}^k \frac{\bar{Q}_{i+1}^k - \bar{Q}_i^k}{\Delta x} \right) + v_{i+1/2}^k}{\left( 1 + g \frac{|v_{i+1/2}^k|}{C_z^2 R_{i+1/2}^k} \right)} \end{aligned}$$

One of the control goals is to maintain the downstream water level to the target level ( $\zeta_t$ ). Therefore, the state is the error between the two levels written as:  $x = \zeta - \zeta_t$ . Because of the symmetry of the first matrix on the left side of Eq. (A.5),  $\zeta$  in the state vector can be simply replaced by  $x$  and the equality function remains (all the water levels along the reach subtract the same target level  $\zeta_t$ ).

## References

- [1] Wahlén BT. Performance of model predictive control on ASCE test canal 1. *J Irrig Drain Eng* 2004;130(3):227–38.
- [2] Willems P, Blanco TB, Chiang PK, Cauwenberghs K, Berlamont J, De Moor B. Evaluation of river flood regulation by means of model predictive control. In: 4th international symposium on flood defence. Managing flood risk, reliability and vulnerability. 2008.
- [3] van Overloop PJ. Model predictive control on open water systems. Delft: IOS Press; 2006.
- [4] Rodellar J, Gomez M, Bonet L. Control method for on-demand operation of open channel flow. *J Irrig Drain Eng* 1993;119(2):225–41.
- [5] Negenborn RR, van Overloop PJ, Keviczky T, De Schutter B. Distributed model predictive control of irrigation canals. *Netw Heterogen Media (NHM)* 2009;4(2):359–80.
- [6] Barjas Blanco T, Willems P, Chiang PK, Haverbeke N, Berlamont J, De Moor B. Flood regulation using nonlinear model predictive control. *Control Eng Pract* 2010;18(10):1147–57.
- [7] Camacho E, Bordons C. Nonlinear model predictive control: an introductory review. Assessment and future directions of nonlinear model predictive control; 2007. p. 1–16.
- [8] Ding Y, Wang SSY. Optimal control of open-channel flow using adjoint sensitivity analysis. *J Hydraul Eng* 2006;132:1215.
- [9] Schwanenberg D, Verhoeven G, Raso L. Nonlinear model predictive of water resources systems in operational flood forecasting. In: 9th international conference on hydroinformatics. HIC 2010, Tianjin, China; 2010.
- [10] Xu M, van Overloop PJ, van de Giesen NC. On the study of control effectiveness and computational efficiency of reduced Saint-Venant model in model predictive control. *Adv Water Res* 2010;34(2):282–90.
- [11] Schittkowski K. NLPQL: A FORTRAN subroutine solving constrained nonlinear programming problems. *Ann Oper Res* 1986;5(1):485–500.
- [12] Chow VT. Open-channel hydraulics. New York: McGraw-Hill Book Co. Inc; 1959.
- [13] Stelling GS, Duinmeijer SPA. A staggered conservative scheme for every Froude number in rapidly varied shallow water flows. *Int J Numer Meth Fluids* 2003;43:1329–54.
- [14] Simon D. Optimal state estimation: Kalman,  $H_\infty$  and nonlinear approaches. New Jersey: John Wiley & Sons, Inc.; 2006.
- [15] Gill PE, Murray W, Wright MH. Practical optimization. London, UK: Academic Press; 1981.
- [16] Han SP. A globally convergent method for nonlinear programming. *J Optim Theory Appl* 1977;22:297.
- [17] Powell MJD. The convergence of variable metric methods for nonlinearly constrained optimization calculations. *Nonlinear Program* 1978;3:27–63.
- [18] Powell MJD. A fast algorithm for nonlinearly constrained optimization calculations. *Numer Anal* 1978;630:144–57.
- [19] Bonnans JF, Gilbert JC, Lemarechal C, Sagastizábal CA. Numerical optimization: theoretical and practical aspects. Springer-Verlag, New York; 2006.
- [20] Sun W, Yuan Y. Optimization theory and methods: nonlinear programming, vol. 1. Springer; 2006.
- [21] Clemmens AJ, Kacerek TF, Grawitz B, Schuurmans W. Test cases for canal control algorithms. *J Irrig Drain Eng* 1998;124(1):23–30.